Research Article Vol. 83, No. 11 / November 2016 / Journal of Optical Technology 673

Journal of Optical Technology

Detection of gas temperature using a distributed feedback laser at O_2 absorption wavelength 760 nm

Z.-R. Zhang,[1,3] P.-S. Sun,[1] H. Xia,[1] Z. Li,[1] T. Pang,[1] B. Wu,[1] X.-J. Cui,[1] and F.-Z. Dong[1,2,4]

[1]Anhui Provincial Key Laboratory of Photonic Devices and Materials, Anhui Institute of Optics and Fine Mechanics, Chinese Academy of Sciences, Hefei 230031, China
[2]School of Environment Science and Optoelectronic Technology, University of Science and Technology of China, Hefei 230026, China
[3]e-mail: zhangzr@aiofm.ac.cn
[4]e-mail: fzdong@aiofm.ac.cn

Received 28 August 2014; Opticheskiĭ Zhurnal **83**, 34–39 (November 2016)

Direct absorption spectroscopy for gas temperature monitoring in a tube furnace is proposed over the temperature range 300–900 K with intervals of 100 K. This detecting technique is based on the relationship between two lines' absorption strength and temperature. The gas temperature can be inferred from the ratio of the integrated spectral area of the oxygen absorption features measured with a distributed feedback diode laser near 760 nm. Compared with the thermocouple measured results, the direct absorption spectroscopy approach also provides a temporal resolution. The results show that the accuracy is better at low temperatures than at high temperatures. In the future, we hope to improve the detection accuracy and demonstrate the utility of the diode laser absorption sensors operating for active combustion diagnostics and optimizations, simultaneously.

OCIS codes: (280.4788) Optical sensing and sensors; (300.6380) Spectroscopy, modulation; (300.1030) Absorption.

https://doi.org/10.1364/JOT.83.000673

1. INTRODUCTION

The determination of parameters in a combustor is generally relevant to the understanding of its combustion progress. Unfortunately, due to extremely harsh combustion environments (high temperature, high dust, and high vapor), many traditional devices, such as thermocouples, have many disadvantages and limited lifetimes [1]. As a result, non-intrusive, remote-sensing diagnostics are desirable for characterizing the parameters at high temperature. Diode laser absorption-based sensors can offer significant opportunities and advantages for making sensitive, selective, and fast *in situ* measurements. Also, these sensors have been developing over the past decade, in such fields as gaseous monitoring [2,3], velocity measurement [4], food safety [5,6], medical diagnosis [7,8], vehicle emission monitoring [9,10], and engine efficiencies [11,12].

This paper will cover the theoretical aspects and the temperature detecting experiments using direct absorption spectroscopy (DAS) techniques.

Molecular oxygen plays a fundamental role in a large variety of natural and industrial processes. Atmospheric transmission in the vicinity of the $O_2 X^3\Sigma_g^- \rightarrow {}^{b1}\Sigma_g^+$ absorption feature near 760 nm is important for remote sensing and military applications. The fast current scanning "finger mark" line capabilities of laser diodes are exploited to achieve gas temperature monitoring in a tube furnace under experimental conditions. In Section 3, the wavelength pair selected rules are denoted. The laser is controlled by homemade circuit boards to lock the absorption wavelength and scanned by the digital signal board. Also, in Section 4, this paper presents the design of the scanned-wavelength temperature sensor for experiments, as demonstrated in a laboratory tube furnace. In Section 5, we present the results of temperature measurements with the main emphasis on the experiment system and algorithm. The details of our initial measurements and preliminary results are discussed.

2. BASIC PRINCIPLE

The fundamental theoretical principle for absorption spectroscopy is the Beer–Lambert law. It describes the relationship between gas concentration X_{abs}, optical length L [cm], and the outgoing $I(\nu)$ and ingoing $I_0(\nu)$ laser light intensities through a gas sample. As Fig. 1 demonstrates, the fractional transmission is

$$\tau_\nu\left(\frac{I(\nu)}{I_0(\nu)}\right) = \exp(-k(\nu)L) = \exp(-PX_{\text{abs}}S(T)\phi(\nu)L), \quad \textbf{(1)}$$

where $k(\nu)$ [cm^{-1}] is the spectral absorption coefficient, which is equivalent to an absorption per unit length, $k(\nu)L$ represents the spectral absorbance, P [atm] is the static gas pressure, and

$\phi(\nu)$ is the gas lineshape function at a frequency of ν. The lineshape function, being normalized, will be unity by definition when integrated across all frequency space:

$$\int_{-\infty}^{+\infty} \phi(\nu)\mathrm{d}\nu = 1.$$

$S(T)$ is the line intensity and can be expressed in terms of known line strength at reference temperature $T_0 \approx 300$ K:

$$S(T) = S(T_0)\frac{Q(T_0)}{Q(T)}\left(\frac{T_0}{T}\right)\exp\left[-\frac{hcE''}{k}\left(\frac{1}{T}-\frac{1}{T_0}\right)\right] \times \frac{1-\exp\left(-\frac{hc\nu_0}{kT}\right)}{1-\exp\left(-\frac{hc\nu_0}{kT_0}\right)}. \quad (2)$$

Except at high T, $\{1 - \exp[-hc\nu_0/(kT_j)]\}$ is very nearly equal to unity and can be neglected, h [6.63×10^{34} J s] is Planck's constant, c [3.0×10^{10} cm/s] is the speed of light, k [1.38×10^{-23} J/K] is Boltzmann's constant, E'' [cm^{-1}] stands for the low state energy for the given wavelength, and $Q(T)$ is the molecular partition function and can be expressed as the following polynomial of temperature:

$$Q(T) = a + bT + cT^2 + dT^3. \quad (3)$$

The coefficients of the polynomial expression for various species are included in the HITRAN08 database [13]. The two-line absorption technique is the most widely used method for temperature measurement in modulation spectroscopy. The gas temperature can be inferred from the measured ratio of integrated absorbance for two different temperature-dependent wavelengths. Because the two integrated absorbances are obtained with the same gas pressure, temperature, and path length, the ratio of these two integrals reduces simply to the ratio of line intensities, which via Eq. (2) is written as

$$T = \frac{\frac{hc}{k}(E_2'' - E_1'')}{\ln\frac{A_1}{A_2} + \ln\frac{S_2(T_0)}{S_1(T_0)} + \frac{hc}{k}\frac{(E_2''-E_1'')}{T_0}}, \quad (4)$$

where hc/k is the constant value 1.438 cm K and A_1 and A_2 are the integrated areas of the absorption lines for DAS. The ratio of the integrated areas of this pair of transitions is only a function of gas temperature:

$$\frac{A_1}{A_2} = \frac{S_1(T)}{S_2(T)}. \quad (5)$$

By measuring the two transitions' integrated absorbance as shown in Fig. 1, temperature can be inferred with Eqs. (4) and (5).

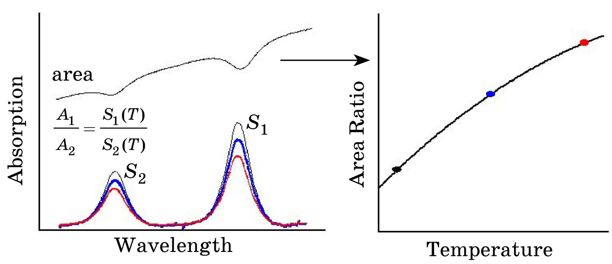

Fig. 1. Temperature inferred from the direct absorption area ratio of line pair transitions.

3. SELECTION OF O_2 PAIRS

Selection of the optimum absorption transitions is the first important step in the development of two-line absorption spectroscopy based on the DAS [14,15]. For this work, we use the HITRAN08 database for sensor design. It contains oxygen vibrational lines in the infrared, and here we concern ourselves with the overtone transitions in the region between 0.5 and 2 pm. The design rules for the line selection are considered as follows.

First, the selected O_2 wavelength should be limited to the near-infrared (NIR) region of 0.7–2 pm, for which fiber-coupled lasers are commercially available at low fiber loss. There are 988 oxygen lines listed in the HITRAN08 database within the above region.

Second, the absorption strength must be large enough to guarantee a good signal-to-noise ratio (SNR). There are 43 oxygen lines selected in step one.

Third, the wavelengths of both absorption lines lie within a single laser scan and should minimize interference from nearby transitions.

Fourth, the line pairs should have sufficiently different line strengths and lower state energies E'' to yield a DAS peak height ratio that is sensitive to temperature, as shown in Fig. 2.

Fifth, the line pair's ratio should be single valued with temperature, and the line strengths should have the same magnitude. If one transition is much stronger or lower, the stronger transition will influence the monitoring of the weak transition. This rule ensures that these two lines have similar SNR [16]. As just described, the selected two-line samples are shown in Fig. 3.

The spectroscopy parameters for the two selected O_2 lines have been systematically measured in a tube furnace for the temperature region of 300–900 K. The selected line pairs can be recorded in a single scan of the diode laser wavelength across about a 0.07 cm^{-1} spectral interval; the selected line transitions are listed in Table 1 (data from Ref. [13]).

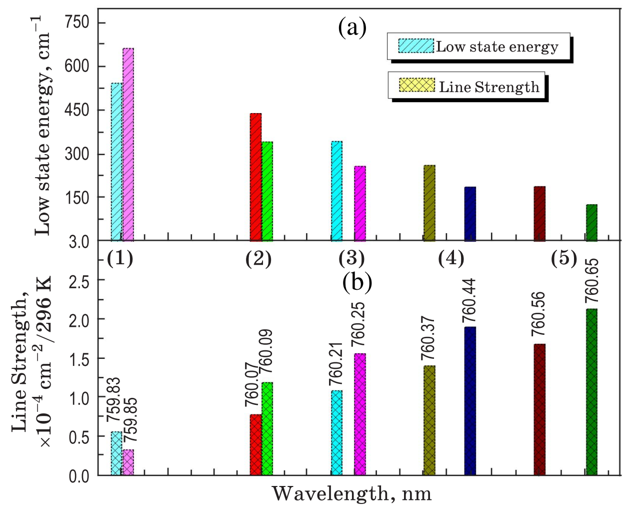

Fig. 2. The five selected oxygen pair lines and low state energy based on the HITRAN08 database. (a) Low state energy and (b) line strength.

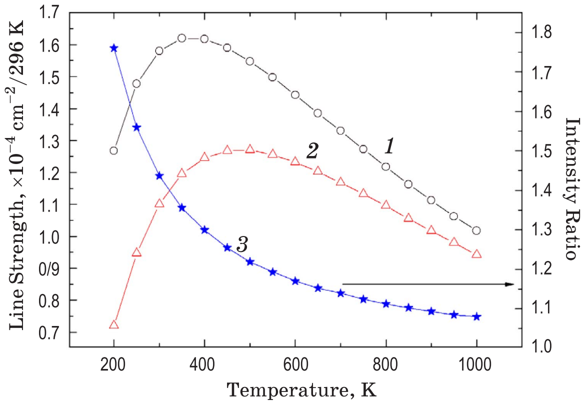

Fig. 3. The scheme of the selected line strengths [wavelength $\lambda_1 =$ 760.26 nm (*1*), wavelength $\lambda_2 =$ 760.21 nm (*2*)] and their ratios (*3*) for temperature.

Table 1. Spectroscopy Parameters for the Selected O_2 Line Pair

λ, nm	Intensity, $cm^{-1}/(mol\,cm^{-2})$ 296 K	E'', cm^{-1}
$\lambda_1 = 760.26$	$6.258E^{-24}$	260.50
$\lambda_2 = 760.21$	$4.337E^{-24}$	345.85

4. CONSIDERATIONS

The absorption spectroscopy technique with modulation had been described in detail elsewhere [17]. In this work the butterfly package distributed feedback diode laser with output in the 760 nm, 2 mW range is used; it is supplied by Nanoplus, Germany. The diode laser is driven by homemade current and temperature controllers to lock the absorption wavelength. The laser is scanned through the two chosen absorption lines by a sawtooth signal at a low frequency of 10 Hz from our designed digital signal board. Also, it was synchronized with the oscilloscope used for data acquisition.

A DAS schematic diagram of the experimental system used for preliminary measurements is shown in Fig. 4. The cell is constructed from a quartz tube (total heated length is 50 cm, inner diameter is 4 cm, and the maximum temperature gradient is determined to be less 0.5%) inserted in an electrically heated cylindrical oven supplied by the Hefei Kejing Materials Technology Co., China. The direct absorption signals are collected by an acquisition card for temperature monitoring extracted from a low-pass filter and a pre-amplifier using one input channel.

The averaging temperature of the absorbing layer is changed by regulation of the electric current of the tube furnace. The strategy for temperature monitoring by DAS is validated over the 300–900 K range with intervals of 100 K. After each step of temperature increase, the temperature stabilized in about 30 min. These measurements are performed inside a tube furnace where the radiative corrections and stability to the thermocouples are minimized within ±10 K errors (see *1*, *2*, and *3* in Fig. 4). In the course of one measurement cycle, the signal is recorded, averaged, and stored in the personal computer memory. As is well known, the SNR increases with the increase of average times. However, considering the response time, sensitivity, and action effect, we used the averaging signals of the 16 scans to analyze and calculate the peak height ratio for temperature monitoring.

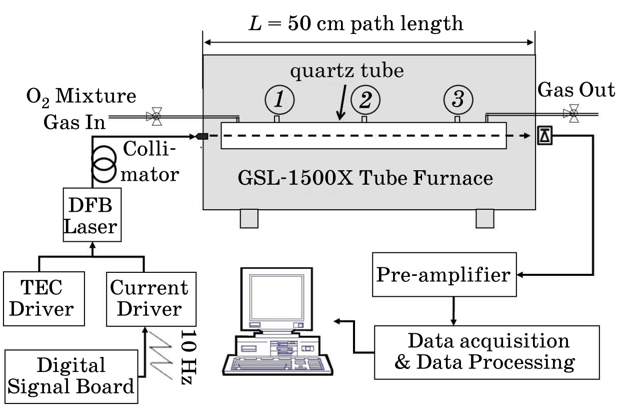

Fig. 4. The experimental schematic of the O_2 temperature measurement system.

5. RESULTS AND DISCUSSION

As discussed above, we presented applications of DAS to monitoring temperatures with an electrical tube furnace at experimental conditions. The example results of an approximately 20% O_2 and N_2 mixture absorption system are discussed in this section.

Figure 5 shows the measurement O_2 absorption spectroscopy of different temperatures at $T =$ 300–900 K. A third-order polynomial fit with non-absorbing wings is performed to extrapolate a zero baseline for the purpose of creating the absorption profiles in different temperatures. Also, the absorption profiles are best-fit using a Lorentz lineshape function and digital smoothing processing. Consequently, the above fitting method introduces some residual noise to the lineshape with

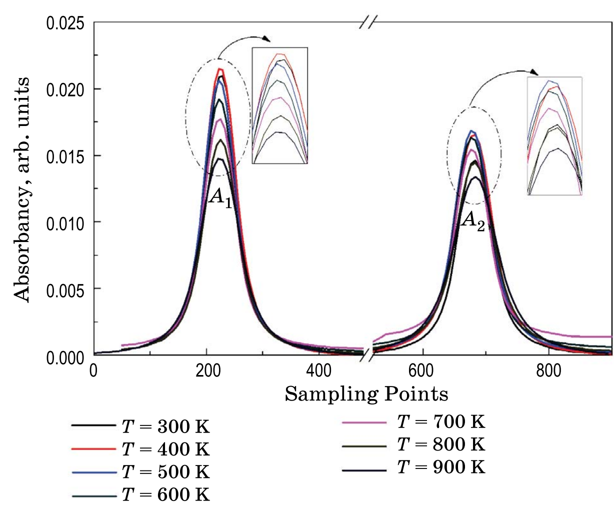

Fig. 5. Expanded view of DAS for the selected O_2 line pair in the 760 nm region.

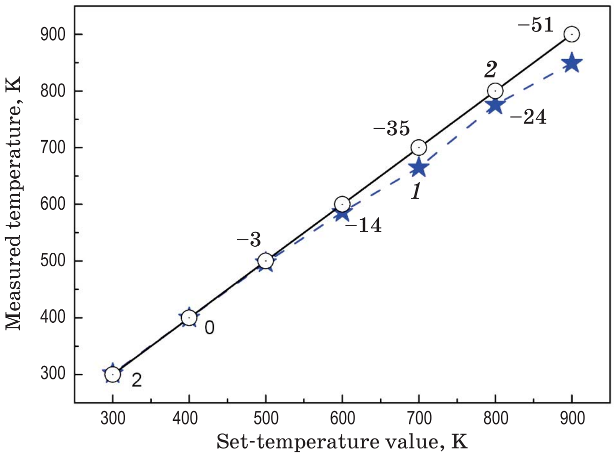

Fig. 6. Comparison of measured temperatures using DAS (*1*) and thermocouple temperatures (*2*).

the temperature increase. In particular, when the absorbing feature is weak, it is difficult to know where the correct nonabsorbing wings of a signal feature begin and end. So the incorrect baseline fits will become sources of measurement errors. Therefore, only small errors for direct absorption measurement will lead to maximum errors at lower gas concentrations.

In Fig. 6, comparison of the measured temperatures and thermocouple data shows good agreement. The abscissa and ordinate are the thermocouple monitoring temperatures and measured temperature values, respectively. The line with stars presents the DAS measured temperatures, and the line with circles presents the thermocouple measured temperatures. The temperatures inferred from the direct absorption profiles are seen to agree extremely well with the thermocouple measurements (max error value is 51 K).

From this graph, we can draw a conclusion that with the increase of gas temperature, the measured temperature errors become more obvious. However, limited to the experimental conditions, we can only assume that the measuring gas pressure is maintained constant. As the case stands, the temperature changes cause the gas pressure to differ, and then cause the absorption broadening to differ, and cause the modulation depth to change, and finally disturb the measured gas temperature's errors, theoretically. In other words, the integrated absorption profiles increase with the gas pressure and decrease with the gas temperature. Under existing laboratory conditions, these factors will be further discussed in future experiments.

6. CONCLUSIONS

Diode laser absorption spectroscopy is applied for the remote measurement of temperature, gas pressure, velocity, and concentration. We have presented an application of DAS to the measurement of gas temperature in the tube furnace. Building on this experiment, temperature strategies based on absorption spectroscopy in more than two lines may then be derived to yield expanded temperature information and therefore enable temperature monitoring in non-uniform conditions.

This procedure greatly simplifies the selection of the most important periods of the industry process. And the spectrometer is easily extendable to other gases such as CO, CO_2, HCl, NH_3, and H_2S by a simple change of laser diode. Therefore, it has the capability to become a universal tool for industrial gas analysis in advanced combustion control applications. It should be noted that the present sensor provides average temperature for a situation in which the temperature distribution along the beam path is uniform. So in future work, the multi-line line-of-sight temperature distributions, gas concentration distributions, and total pressure will be inferred from the dynamic absorption spectral division with the "CT" model and complicated algorithms to investigate the detailed internal situations.

Funding. National Natural Science Foundation of China (NSFC) (11204320, 41405034, 11204319); National Key Technology Research and Development Program of the Ministry of Science and Technology (MOST) of China (2014BAC17B03); Basic Research on Scientific Instruments of the Chinese Academy of Sciences (CAS) (YZ201315); CAS President's International Fellowship Initiative (PIFI) (2015VMA007).

REFERENCES

1. J. R. Veale, L. G. Wang, and T. F. Gallagher, "Remote sensing of O_2 in a supersonic combustor using diode lasers and fiber optics," in *4th Symposium on Multidisciplinary Analysis and Optimization* (AIAA, Cleveland, Ohio, 1992), paper 5090.
2. F. D. Amato, H. P. Mazzing, and F. Castagnoli, "Methane analyzer based on TDL's for measurements in the lower stratosphere: design and laboratory tests," Appl. Phys. B **75**(2), 195–202 (2002).
3. G. C. Sauer, T. J. Pisano, and R. D. Fitz, "Tunable diode laser absorption spectrometer measurements of ambient nitrogen dioxide, nitric acid, formaldehyde, and hydrogen peroxide in Parlier, California," Atmos. Environ. **37**, 1583–1591 (2003).
4. F. Li, X. L. Yu, W. W. Cai, and L. Ma, "Uncertainty in velocity measurement based on diode-laser absorption in nonuniform flows," Appl. Opt. **51**(20), 4788–4797 (2012).
5. M. Lewander, Z. G. Guan, L. Persson, A. Olsson, and S. Svanberg, "Food monitoring based on diode laser gas spectroscopy," Appl. Phys. B **93**(2–3), 619–625 (2008).
6. U. Tylewicz, P. Lundin, L. Cocola, K. Dymek, P. Rocculi, S. Svanberg, P. Dejmek, and F. Gomez Galindo, "Gas in scattering media absorption spectroscopy detected persistent vacuum in apple tissue after vacuum impregnation," Food Biophys. **7**(1), 28–34 (2012).
7. C. Roller, K. Namjou, and J. Jeffers, "Simultaneous NO and CO_2 measurement in human breath with a single IV–VI mid-infrared laser," Opt. Lett. **27**(2), 107–109 (2002).
8. M. R. McCurdy, Y. Bakhirkin, G. Wysocki, R. Lewicki, and F. K. Tittel, "Recent advances of laser-spectroscopy-based techniques for applications in breath analysis," J. Breath Res. **1**(1), 014001 (2007).
9. F. Z. Dong, W. Q. Liu, J. G. Liu, X. H. Tu, Y. J. Zhang, F. Qi, P. H. Xie, Y. H. Lu, S. M. Wang, Y. P. Wang, and Q. N. Wei, "On-line roadside vehicle emissions monitoring (Part I)," J. Test Meas. Technol. **19**(2), 110–120 (2005).
10. F. Z. Dong, W. Q. Liu, J. G. Liu, X. H. Tu, Y. J. Zhang, F. Qi, P. H. Xie, Y. H. Lu, S. M. Wang, Y. P. Wang, and Q. N. Wei, "On-line roadside vehicle emissions monitoring (Part II)," J. Test Meas. Technol. **19**(3), 237–244 (2005).
11. J. L. Bradshaw, J. D. Bruno, K. M. Lascola, R. P. Leavitt, J. T. Pham, F. J. Towner, D. M. Sonnenfroh, and K. R. Parameswaran, "Small, low-power consumption CO-sensor for post-fire cleanup aboard spacecraft," Proc. SPIE **8032**, 80320D (2011).

12. A. D. Sappey, P. Masterson, E. Huelson, J. Howell, M. Estes, H. Hofvander, and A. Jobson, “Results of closed-loop coal-fired boiler operation using a TDLAS sensor and smart process control software combustion,” Sci. Technol. **183**(11), 1282–1295 (2011).
13. L. S. Rothman, I. E. Gordon, A. Barbe, D. C. Benner, P. F. Bernath, M. Birk, V. Boudon, L. R. Brown, A. Campargue, J. P. Champion, K. Chance, L. H. Coudert, V. Dana, V. M. Devi, S. Fally, J. M. Flaud, R. R. Gamache, A. Goldman, D. Jacquemart, I. Kleiner, N. Lacome, W. J. Lafferty, J. Y. Mandin, S. T. Massie, S. N. Mikhailenko, C. E. Miller, A. N. Moazzen, O. V. Naumenko, A. V. Nikitin, J. Orphal, V. I. Perevalov, A. Perrin, C. A. Predoi, C. P. Rinsland, M. Rotger, M. Simeckova, M. A. H. Smith, K. Sung, S. A. Tashkun, J. Tennyson, R. A. Toth, A. C. Vandaele, and A. J. Vander, “The HITRAN 2008 molecular spectroscopic database,” J. Quant. Spectrosc. Radiat. Transfer **110**(9–10), 533–572 (2009).
14. X. Zhou, X. Liu, J. B. Jeffries, and R. K. Hanson, “Development of a sensor for temperature and water concentration in combustion gases using a single tunable diode laser,” Meas. Sci. Technol. **14**(8), 1459–1468 (2003).
15. X. Zhou, J. B. Jeffries, and R. K. Hanson, “Development of a fast temperature sensor for combustion gases using a single tunable diode laser,” Appl. Phys. B **81**(5), 711–722 (2005).
16. V. Nagali and R. K. Hanson, “Design of a diode-laser sensor to monitor water vapor in high-pressure combustion gases,” Appl. Opt. **36**(36), 9518–9527 (1997).
17. D. E. Cooper and R. E. Warren, “Frequency modulation spectroscopy with lead-salt diode lasers: a comparison of single-tone and two-tone techniques,” Appl. Opt. **26**(17), 3726–3732 (1987).